Plastic Deformation of Spinning Iron Whiskers

W. L. Piotrowski, D. C. Larson, and J. W. Beams

Citation: Journal of Applied Physics **37**, 3153 (1966); doi: 10.1063/1.1703177
View online: https://doi.org/10.1063/1.1703177
View Table of Contents: http://aip.scitation.org/toc/jap/37/8
Published by the American Institute of Physics

Plastic Deformation of Spinning Iron Whiskers*

W. L. Piotrowski, D. C. Larson, and J. W. Beams
Department of Physics, University of Virginia, Charlottesville, Virginia
(Received 4 March 1966)

Single-crystal iron whiskers are plastically deformed centrifugally with no gripping constraints. A calculation of the stresses in a rotating body with a square cross section is given which allows a determination of the resolved shear stresses in the whiskers at their yield points. The stresses obtained are intermediate between the bulk values and the smaller whisker values as expected. The average critical resolved shear stress was 6.8 kg/mm^2 for all the whiskers except three which yielded at a somewhat lower stress of 4.1 kg/mm^2. For whisker widths ranging from 310 to 820 μ, no systematic dependence of yield stress on size was found.

INTRODUCTION

CONSIDERABLE interest in the mechanical properties of metallic whiskers has arisen since the discovery that the strength of some whiskers approaches the theoretical strength of perfect crystals.[1] A typical instrument for measuring the tensile properties of whiskers is a form of analytical balance in which one arm is used for supporting the load train and the other arm is used for the application of stress. The specimen is attached to the load train by a thermal cement. Using this type of device, whiskers shorter than about 2 mm cannot be tested since a certain length of the specimen must be used to attach it to the load train. When the whisker is attached by a cement, the process of the cement cooling and setting introduces stresses into the whiskers, the magnitude of which is unknown. If a normal tensile testing machine is used, the process of clamping the whiskers in the grips also introduces unknown stresses. The method used in the present experiments can be used with whiskers of less than 2 mm of length, and there are no stresses due to the gripping constraints.

In investigations of physical phenomena associated with high centrifugal fields, one of us[2] has magnetically suspended small ferromagnetic rotors and spun them to high angular velocities. Since iron whiskers are ferromagnetic, the same technique used in determining the strength of small ferromagnetic rotors is applicable to iron whiskers. It is the purpose of the present paper to report on some experiments on the deformation of iron whiskers which are magnetically suspended inside an evacuated chamber and spun. The only forces acting on the crystal are the gravitational force which is negligible and the centrifugal force due to the spinning motion of the whisker; there are no grip constraints. In addition the elastic stress distribution in a rotating whisker is calculated. This calculation allows a comparison of the present results with those obtained in previous iron whisker experiments[3] and with experiments on bulk iron single crystals.[4]

EXPERIMENTAL PROCEDURE

Single crystal α-iron whiskers were grown by the hydrogen reduction of ferrous chloride. The experimental growth procedure, the size of the crystals, and the crystal orientations have been described in detail in the literature.[5,6] The whiskers selected for the present investigation had a ⟨100⟩ longitudinal axis and a square cross section.

If a rotor or a whisker is magnetically suspended and rotated about a principal axis, this motion is stable when the rotation is about the axis of largest moment of inertia and metastable about any other axis. For this reason the whiskers used in these tests were cut to lengths where the maximum moments of inertia would be around ⟨100⟩ spin axes; the whiskers were cut to their final cubic shape with a centrifugal acid saw.[7] This procedure eliminated troublesome flexural vibrations, since the fundamental vibration frequencies were well above the rotor bursting frequency. If the mechanical strength of long filamentary crystals is to be determined using the centrifugal technique, it is preferable that a stable rotor be used as a carrier vehicle for the whiskers.

The cube-shaped specimen (rotor) is placed in a Pyrex glass chamber which is connected to a vacuum system and suspended magnetically. Acceleration of the rotor is accomplished by producing a magnetic field rotation in a plane normal to the axis of the support field. Eddy currents, induced in the rotor by this field, react with the field to produce a torque on the rotor. The driving field is obtained by placing two coils perpendicular to each other around the rotor and passing an alternating current through the coils so that the current through one coil is 90° out of phase with that through the other. Determination of the rotor

* This work was supported by a grant from the Army Office of Research, Durham, North Carolina.

[1] C. Herring and J. K. Galt, Phys. Rev. **85**, 1060 (1952).

[2] J. W. Beams, Physics Today **12**, 20 (1959), and references cited therein.

[3] S. S. Brenner, J. Appl. Phys. **27**, 1484 (1956).

[4] N. P. Allen, B. E. Hopkins, and J. E. McLennan, Proc. Roy. Soc. (London) **A234**, 221 (1956).

[5] R. V. Coleman, J. Appl. Phys. **29**, 1487 (1958).

[6] S. S. Brenner, Acta Met. **4**, 62 (1956).

[7] W. L. Piotrowski and J. W. Beams, Rev. Sci. Instr. **35**, 1726 (1964).

speed is accomplished by focusing a beam of light from a dc light source onto the surface of the rotor. The reflected light passes into a Lucite light pipe and into a photomultiplier tube. The output of the photomultiplier is applied to the verical deflection plates of an oscilloscope and an audio oscillator is connected to the horizontal input. The angular speed of the rotor is then determined from the Lissajous pattern displayed on the cathode ray tube.

When the crystal begins to flow plastically, conservation of angular momentum requires that the angular velocity of the rotor decrease. This is readily observable on the oscilloscope and consequently the angular velocity corresponding to the yield stress may be very accurately determined. The rotor will then continue to deform until it is no longer dynamically stable or until it fractures at which time it will come out of support.

RESULTS

Eleven iron single-crystal whiskers ranging in width from 310 to 820 μ were successfully tested by the centrifugal technique. Three different modes of deformation were observed.

Slow Plastic Deformation

Four crystals ranging in width from 405 to 820 μ were observed to undergo a slow plastic deformation. A typical example is a crystal of width 700 μ which was driven to a maximum angular frequency of 90 000 cps (rev/sec). When the crystal reached this frequency, the acceleration ceased although power continued to be applied to the drive coils, and therefore, a torque was still applied to the crystal. The angular velocity of the crystal remained constant for 25 min and then the rotor began to decelerate at 1000 cps/min. At an angular frequency of 68 000 cps the crystal had deformed to such an extent that it was no longer dynamically stable and it came out of the support. A drawing of the general shape of the deformed crystal is shown in Fig. 1. It has roughly the appearance of a "dogbone." Two sets of slip lines were visible on the sides of the crystal and one set of slip lines was visible on the top and bottom of the crystal (normal to the axis of rotation.) The observed slip lines are shown schematically in Fig. 1.

Rapid Plastic Deformation

The second type of deformation that frequently occurs is quite similar to that previously described. Slip seems to occur on the same slip systems. In this case, however, the crystal deforms mainly in the center where it necks down and separates, but the rest of the crystal is relatively free of plastic deformation. The crystals fail in a ductile manner and no brittle fractures are observed. Three crystals varying in width between 450 and 600 μ were observed to rupture in this manner. The elapsed time from the point at which the acceleration of the crystal began to decrease until it ruptured was about one minute.

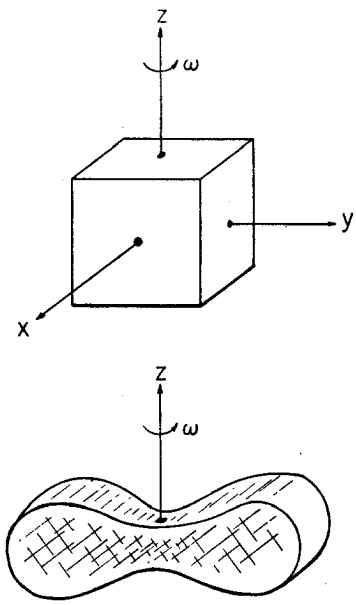

FIG. 1. Top: Underformed single-crystal iron cube. Bottom: General appearance of cubic crystal after plastic deformation. The dominent slip lines are shown schematically.

Complex Deformation

Two crystals failed when a corner of the cube sheared off suddenly from the rest of the crystal. Two other crystals deformed in a complex manner with the formation of deformation bands. The final deformed shape of these crystals was quite irregular.

DISCUSSION

Yield Stresses

The yield point of the spinning whiskers is the point at which the acceleration of the whisker ceases. This results from the fact that the rotor friction is very small, which permits the torque produced by the rotor drive to be small. Consequently a small change in the moment of inertia due to deformation reduces the rotor speed or prevents further acceleration. The frequency at yield was very accurately determined for each of the whiskers tested. The yield stress corresponding to this frequency may be calculated from the theoretical stress distribution if the slip system which operates initially is known. The stress distribution in an isotropic rotating body with a square cross section is given in the Appendix. Using these results it is easy to calculate the resolved shear stress on any of the possible slip systems. The operative slip systems in iron at room temperature are normally {110} ⟨111⟩, {211} ⟨111⟩, and {321} ⟨111⟩. In most of the whiskers, the most obvious slip lines corresponded to the {110} planes which were parallel to the x and y axes (see Fig. 1). Consequently the resolved shear stresses were calculated on the assumption that slip was initiated on these planes. In Table I the values calculated for the maximum resolved shear stresses are given along with

TABLE I. Summary of deformation data.

Crystal width (μ)	Mode of deformation	Frequency at failure (kc/sec)	Critical resolved shear stress (kg/mm^2)
405	Slow	160	7.5
620	Slow	97	6.5
700	Slow	90	7.1
820	Slow	65	5.1
450	Rapid	110	4.4
510	Rapid	90	3.8
600	Rapid	81	4.2
310	Complex	205	7.2
460	Complex	135	6.9
480	Complex	130	7.0
550	Complex	116	7.3

the width, mode of deformation, and frequency at the yield point for the eleven whiskers. The maximum stresses occur as expected along the axis of rotation. The yield stresses for the whiskers which exhibited a rapid deformation were found to range from 3.8 to 4.4 kg/mm^2 with an average value of 4.1 kg/mm^2 while the yield stresses for the other whiskers ranged from 5.1 to 7.5 kg/mm^2 with an average value of 6.8 kg/mm^2. Consequently it appears that the whiskers which suffered a rapid deformation may have had internal flaws which led to premature failure. The yield shear stresses obtained for these whiskers with widths ranging from 310 to 820 μ are greater than those obtained with bulk iron single crystals and are less than those obtained with very small whiskers. Brenner[3] obtained values of about 20–25 kg/mm^2 for whiskers of width about 15 μ, and Allen *et al.*[4] obtained an average value of 3.7 kg/mm^2 for bulk iron single crystals. No dependence of yield stress on size was found for whiskers of widths ranging from 310 to 820 μ.

Plastic Deformation

After the yield point is reached, the whiskers begin to plastically deform and the angular velocity either remains constant or it begins to slowly decrease. Finally, the deformation is so severe that the rotor becomes unstable and drops from the suspension. For the case of slow plastic deformation the final shape of the crystal is a dumbbell as shown in Fig. 1. For this type of deformation the slip occurs primarily on two planes: the (011) and (01$\bar{1}$). The resolved shear stress on these planes in the ⟨111⟩ directions has a maximum value of $0.23\rho\omega^2a^2$ along the axis of rotation of the whisker, an intermediate value of $0.1\rho\omega^2a^2$ at the points $x=\pm a$, $y=0$, and 0 at the points $x=0$, $y=\pm a$; the width of the whisker is $2a$. Therefore, slip very likely is initiated at the center and propagated in the x direction. The deformed shape of the crystal seems to support this interpretation.

The initiation of slip on the (011) and (01$\bar{1}$) planes seems to prevent the development of slip on the (101) and (10$\bar{1}$) planes. This phenomena of latent hardening is quite common in single-crystal deformation experiments where multiple slip occurs. If all of the equally stressed slip systems were to slip an equal amount, the deformed crystals would have four-fold symmetry with respect to the z axis rather than the observed two-fold symmetry. The resolved shear stresses on the planes (110) and (1$\bar{1}$0) in the ⟨111⟩ directions are also calculated in the Appendix. The maximum stress occurs along the midpoints of the cube edges and has a value of $0.14\rho\omega^2a^2$. This is considerably less than the shear stresses calculated for the other slip systems. As expected, slip lines corresponding to these planes were not observed.

The deformed shapes of the crystals which underwent a rapid plastic deformation were quite similar to those above and the deformation proceeded in a similar manner. The deformation of the crystals which exhibited a complex deformation cannot be simply interpreted.

ACKNOWLEDGMENTS

We wish to express our appreciation to Dr. J. W. Mitchell for making available his optical and x-ray equipment and to Dr. R. V. Coleman for assistance in the growth of some of the iron whiskers.

APPENDIX

The elastic stresses in a rotating body with a square cross section may be calculated approximately using the Principle of Least Work. The body will be assumed to be isotropic and linear and the plane stress approximation will be used. The plane strain approximation requires that the z displacements (parallel to the rotation axis) be negligible which is contrary to what is observed experimentally. The plane stress solutions are strictly applicable to only a thin plate but will apply approximately to the cube-shaped crystal considered here. The solution to the problem can be written as a superposition of (a) an inhomogeneous solution of the equilibrium equations for a centrifugal body force (this reduces the problem to an ordinary boundary value problem); (b) an adjustment solution which eliminates the surface shear stresses; and (c) a solution for a square plate which has a parabolic distribution of edge tractions.

If a body of uniform density ρ rotates with constant angular velocity ω about the z axis; the stresses which satisfy the equilibrium equations are given as

$$\begin{aligned} \sigma_{xx} &= -(A+B)x^2 - Ay^2, \\ \sigma_{yy} &= -(A+B)y^2 - Ax^2, \\ \sigma_{xy} &= -Bxy, \end{aligned} \tag{1}$$

where $A=(1+2\nu)\rho\omega^2/8(1-\nu)$, $B=(1-2\nu)\rho\omega^2/4(1-\nu)$, and ν is Poisson's ratio.

If we consider the body to have a square cross section of edge of length $2a$, a solution which eliminates the

shear stresses of Eq. (1) may be obtained from a fourth-order Airy's stress function:

$$\sigma_{xx}=B(y^2-x^2)/2+a^2(2A+B),$$
$$\sigma_{yy}=B(x^2-y^2)/2+a^2(2A+B), \quad (2)$$
$$\sigma_{xy}=Bxy.$$

The sum of the solutions (1) and (2) gives a normal stress along the edges $x=\pm a$ of $\sigma_{xx}=(A-B/2)(a^2-y^2)$ and a normal stress along the edges $y=\pm a$ of $\sigma_{yy}=(A-B/2)(a^2-x^2)$. A solution to the problem of a square plate with the above parabolic surface stress distributions (with opposite sign) has been given by Timoshenko[8] using the Principle of Least Work:

$$\sigma_{xx}=-(2A-B)(a^2-y^2)/2-4(x^2-a^2)^2[2\alpha_1(3y^2-a^2)+\alpha_2(15y^4-12a^2y^2+6x^2y^2-2a^2x^2+a^4)],$$

$$\sigma_{yy}=-(2A-B)(a^2-x^2)/2-4(y^2-a^2)^2[2\alpha_1(3x^2-a^2)+\alpha_2(15x^4-12a^2x^2+6x^2y^2-2a^2y^2+a^4)], \quad (3)$$

$$\sigma_{xy}=16xy(x^2-a^2)(y^2-a^2)[2\alpha_1+\alpha_2(3x^2+3y^2-2a^2)],$$

where

$$\alpha_1=0.0404(2A-B)/2a^4$$

and

$$\alpha_2=0.01174(2A-B)/2a^6.$$

The final solution for the stresses in a rotating cube is the sum of Eqs. (1)–(3). Using this solution it is now possible to calculate the resolved shear stresses on the 12 {110} ⟨111⟩ slip systems, the 12 {211} ⟨111⟩ slip systems, and the 24 {321} ⟨111⟩ slip systems. The maximum resolved shear stress on the {110} planes (in ⟨111⟩ directions) parallel to the x and y axes is $\sigma=0.22\times\rho\omega^2a^2$ and the maximum resolved shear stress on the {110} planes parallel to the z axis is $\sigma=0.14\rho\omega^2a^2$.

[8] S. Timoshenko, Phil. Mag. 47, 1095 (1924).

JOURNAL OF APPLIED PHYSICS VOLUME 37, NUMBER 8 JULY 1966

Direct $^2T_1$–^2E Phonon Relaxation in Ruby and Its Effect Upon R-Line Breadth

JOSEPH A. CALVIELLO, EDWARD W. FISHER, AND ZINDEL H. HELLER
Airborne Instruments Laboratory, Division of Cutler-Hammer, Inc., Melville, Long Island, New York
(Received 7 January 1966; in final form 14 March 1966)

Fluorescence spectroscopy and R-line excitation measurements have been made on ruby samples at 4°K. These demonstrate the existence of a direct relaxation process between the $^2T_1$ and ^2E levels—possibly by emission of a phonon into a mode affecting the trigonal component of the chromium ion site symmetry. It is shown that this process contributes a substantial part to the temperature-dependent R-line breadth in the range 100°–500°K.

INTRODUCTION

WE have shown that the ruby R lines can be excited in a sample at liquid-helium temperature by optical pumping of the $^2T_1$ levels. Moreover, the yield for this process varies very little over the temperature range 4°–300°K. Therefore, there must be an allowed nonradiative $^2T_1\rightarrow{}^2E$ transition, which is responsible for establishing thermal equilibrium between these multiplets. The total optical breadth of the lower $^2T_1$ sublevel (14 950 cm^{-1}) is shown to arise from this downward transition and part of the ^2E breadth can also be attributed to lifetime shortening caused by the inverse process. The breadth of the upper $^2T_1$ sublevels (15 180 cm^{-1}) is shown from optical data and relaxation rates calculated from strain data to be caused by nonradiative transitions to the lower $^2T_1$ sublevel rather than to ^2E; evidently the latter mechanism is not permitted.

BACKGROUND

Figure 1 shows the pertinent energy levels of the Cr^{+++} ion in ruby,[1] and their dependence upon the cubic field parameter Dq/B. The principal perturbation to the free-ion states occurs through the predominantly cubic crystalline Stark field.[2] At the value of $Dq/B\approx3$ prevailing at the Cr^{+++} ion site in ruby, the spacings between the $^2T_2$, $^2T_1$, ^2E, and $^4A_2$ levels are essentially constant. The $^4T_2$ and $^4T_1$ energy levels vary strongly with Dq/B, converging towards the lower-lying energy levels as Dq/B is reduced. The ^2E and $^2T_1$ multiplets are separated from the $^4A_2$ ground state by about 14 400 cm^{-1} and 15 000 cm^{-1}, respectively; the $^4T_2$ band extends between 16 500 cm^{-1} and 21 000 cm^{-1} above the ground state.

The small trigonal field component in ruby[3] interacts with the spin–orbit coupling to split the ^2E level into a pair of Kramer's doublets spaced by 30 cm^{-1} and the $^2T_1$ level[4] into 3 Kramer's doublets as shown. It also produces small electric dipole moments for transitions from these levels to the ground state, resulting in radiative lifetimes of about 3×10^{-3} sec from the ^2E levels, the R lines, and 10×10^{-3} sec from the $^2T_1$ levels,

[1] D. F. Nelson and M. D. Sturge, Phys. Rev. 137, A1117 (1965).

[2] Y. Tanabe and S. Sugano, J. Phys. Soc. Japan 9, 766 (1954).
[3] Y. Tanabe and S. Sugano, J. Phys. Soc. Japan 13, 880 (1958).
[4] J. Margerie, Compt. Rend. 225, 1598 (1962).